

Supporting Information

Towards Predictive Control of Reversible Nanoparticle Assembly with Solid-Binding Proteins

Yifeng Cai,^a Xin Qi,^a Julia Boese,^a Yundi Zhao,^a Brittney Hellner,^a Jaehun Chun,^{b,c}
Christopher J. Mundy,^{a,b} and François Baneyx*^a

^aDepartment of Chemical Engineering, University of Washington, Seattle, Washington 98195, United States. ^bPhysical and Computational Sciences Directorate, Pacific Northwest National Laboratory, Richland, Washington 99354, United States. ^cLevich Institute and Department of Chemical Engineering, CUNY City College of New York, New York, New York 10031, United States

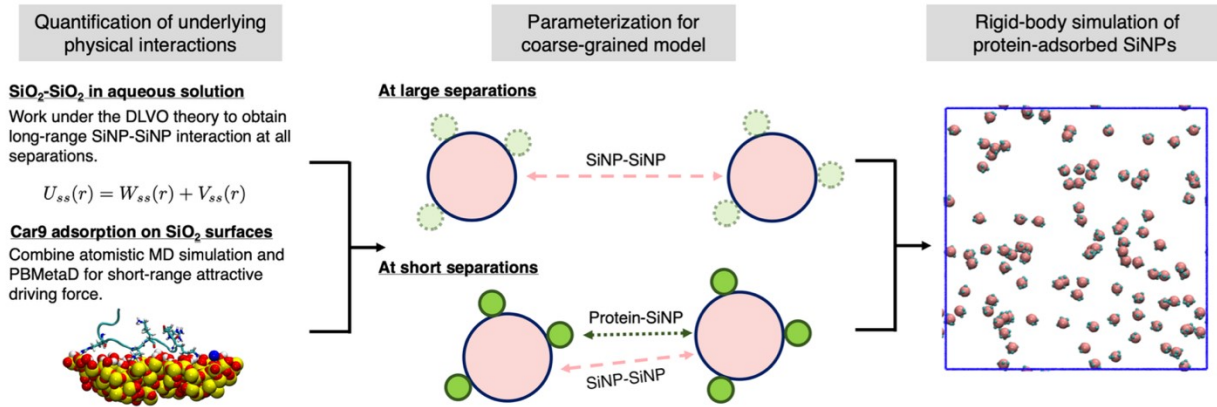


Fig. S1 Our multiscale simulation framework combines top-down and bottom-up approaches to model the assembled state of silica nanoparticles by bifunctional solid-binding proteins. See ref. [1] for details.

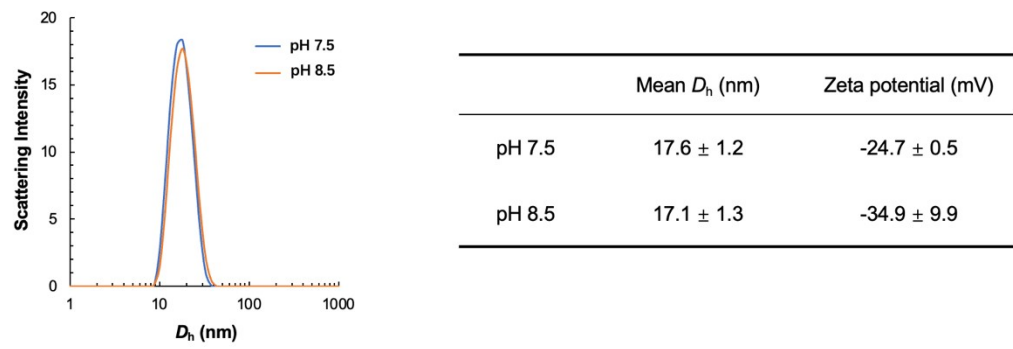


Fig. S2 Size distributions and zeta potentials of bare SiNP at pH 7.5 and pH 8.5.

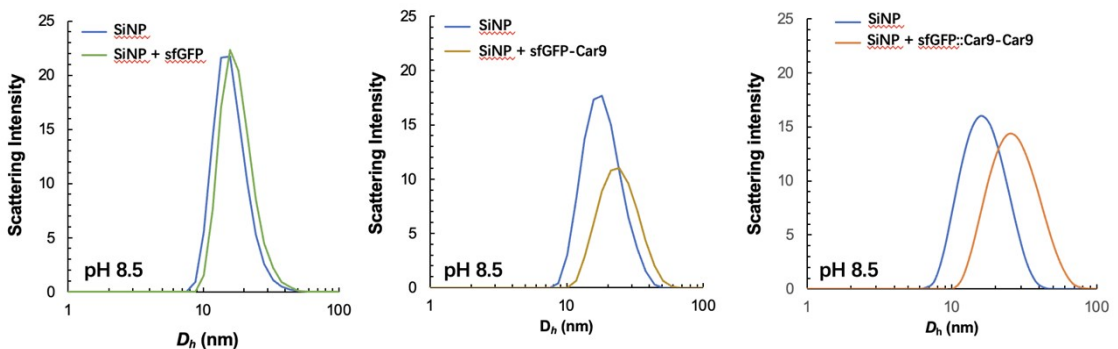


Fig. S3 Size distribution of bare SiNP at pH 8.5 (blue curves) and in the presence of a 5:1 molar excess of wild type sfGFP (gold curve, center panel) or sfGFP::Car9-Car9 (orange curve). The D_h progressively increases from about 17 nm for bare SiNPs, to 24 nm for SiNPs decorated with a sfGFP-Car9 shell, to about 28 nm for SiNPs decorated with the sfGFP::Car9-Car9 bifunctional protein.

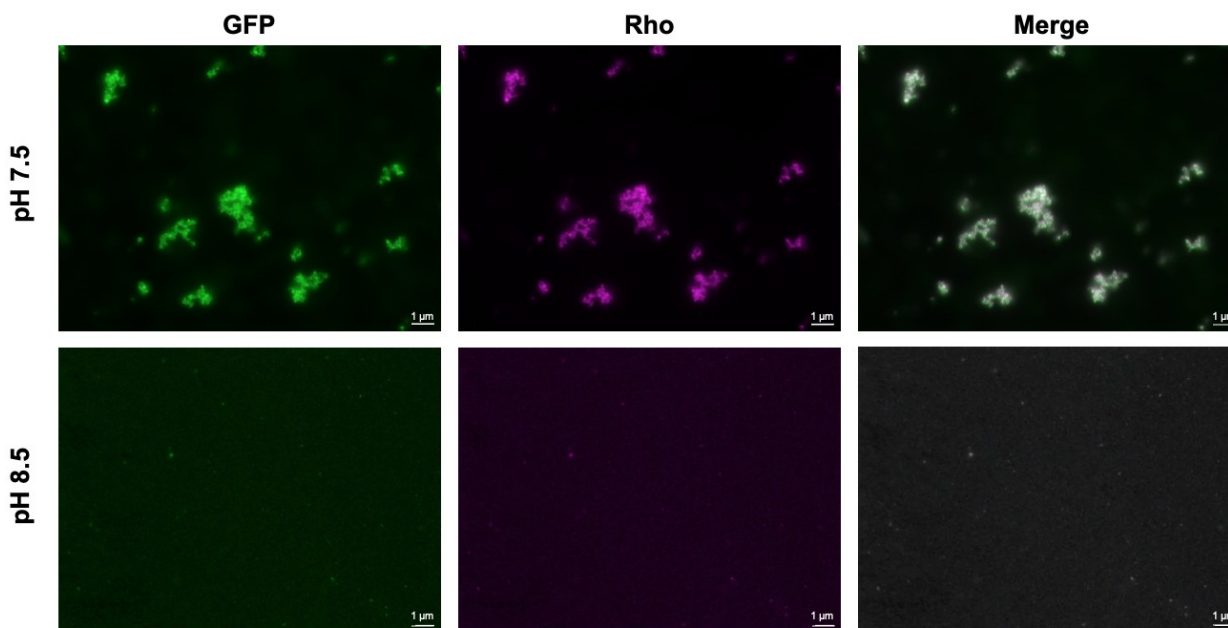


Fig. S4 Fluorescence microscopy images of the self-assembled clusters obtained at pH 7.5 (top), and of the dispersed, protein-bound SiNP obtained by shifting the pH to 8.5 (bottom). sfGFP::Car9-Car9 was mixed with SiNP at a 5:1 molar equivalent ratio and images were acquired at the indicated pH in the GFP (sfGFP fluorescence, left panels) and Rhodamine (rhodamine molecules encapsulated within the SiNPs, middle panels) channels of the microscope. Artificially colored images were merged (right panels) to demonstrate colocalization.

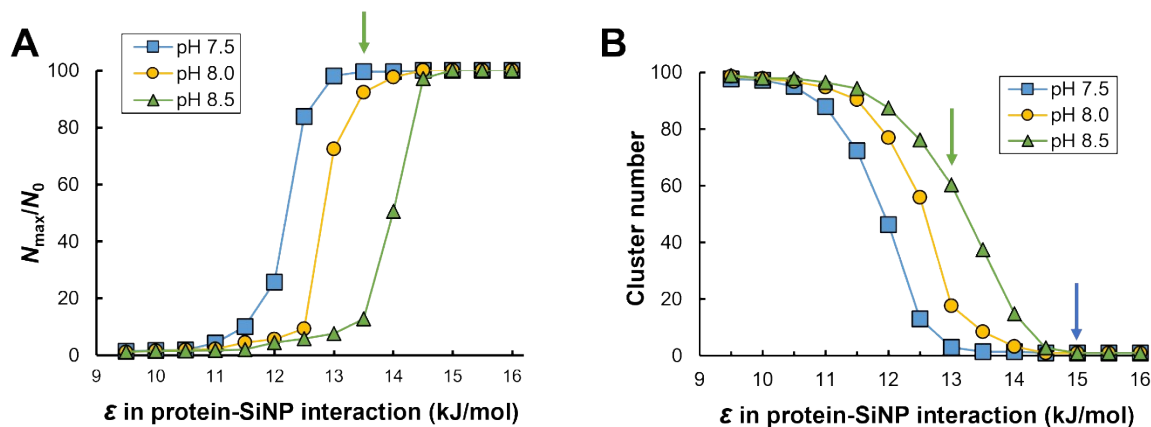


Fig. S5 (A) Evolution of the assembled state N_{max}/N_0 with the depth of the protein-SiNP attractive potential. Rigid body simulations were conducted at a 5:1 molar equivalent of sfGFP::Car9-Car9 to 10 nm SiNPs and at the indicated pH. Data at pH 7.5 and pH 8.5 is taken from Fig. 4 in reference 1. **(B)** Number of clusters present in the last 500 frames of each simulation as a function of ϵ . The green and blue arrows indicate the precise value of ϵ at pH 8.5 and 7.5, respectively.

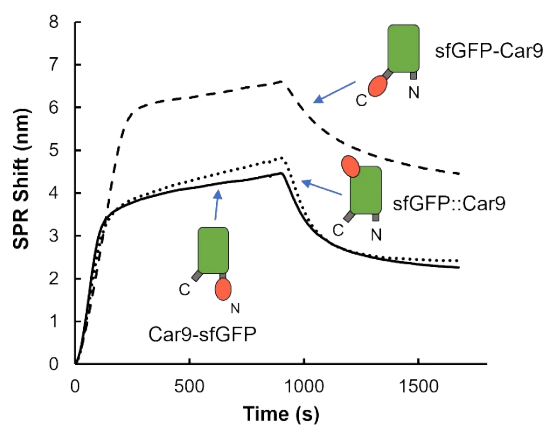


Fig. S6 Influence of the Car9 insertion point on silica-binding affinity by monofunctional sfGFP derivatives. SPR sensorgrams were collected at pH 7.5, a protein concentration of 100 μ M, and a flowrate of 70 μ L/min using silica-coated chips and as described in reference 2. Equilibrium SPR shifts approximates protein coverage. A wash phase in which protein-free buffer is flowed over the chips starts at $t = 900$ s.

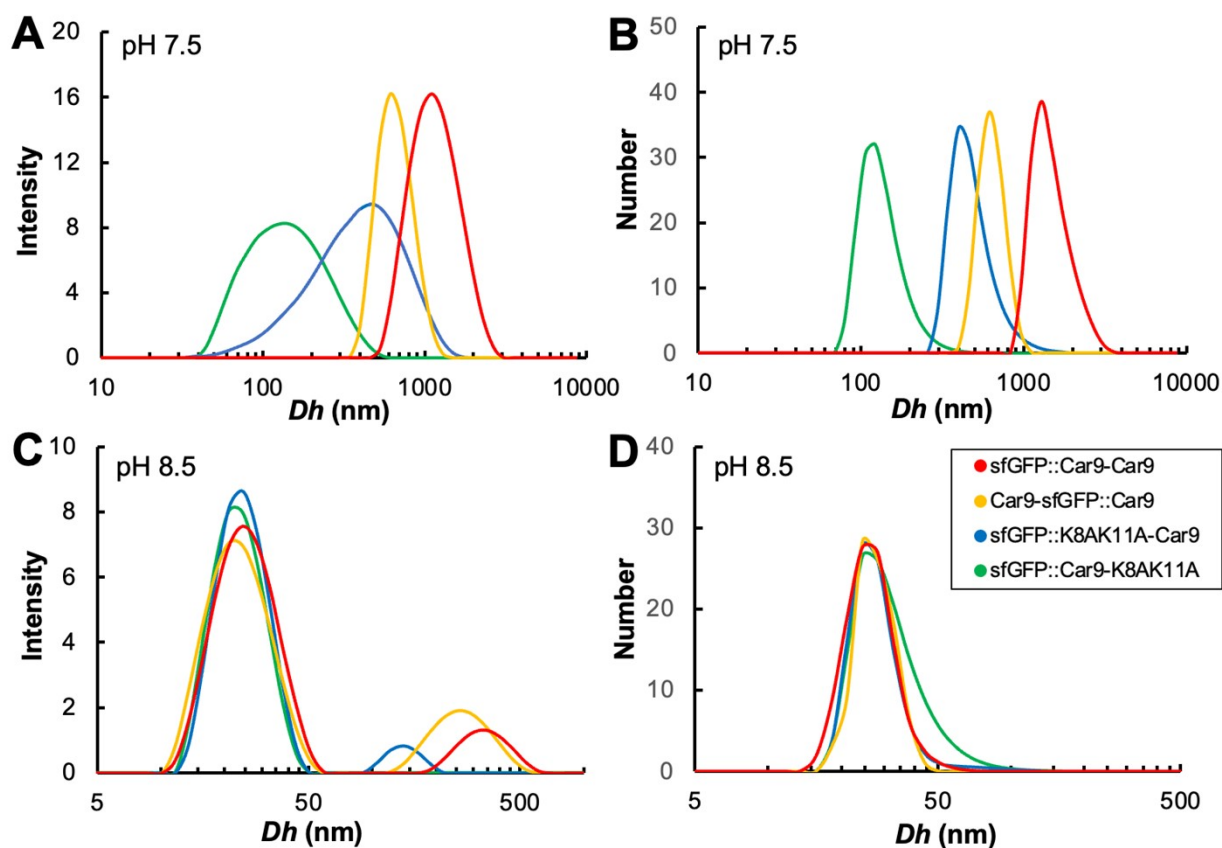


Fig. S7 Size distributions based on scattering intensity (**A**, **C**) or particle numbers (**B**, **D**) were obtained by DLS upon mixing the indicated bifunctional sfGFP constructs with 10 nm SiNP at a 5:1 molar equivalent. Samples prepared at pH 7.5 (**A**, **B**), were shifted to pH 8.5 by addition of NaOH (**C**, **D**).

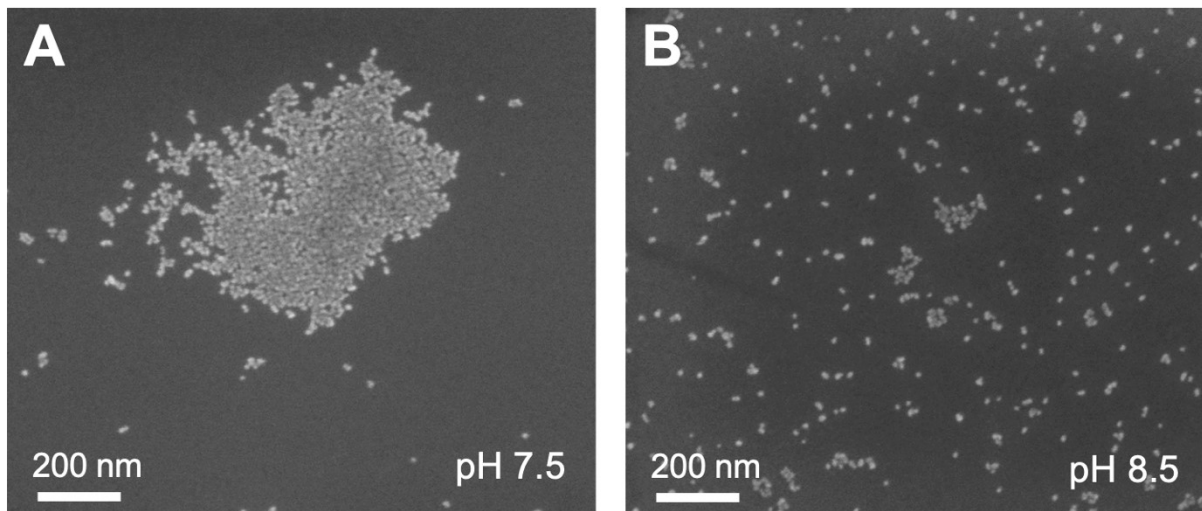


Fig. S8 Representative SEM images of samples obtained upon mixing a 5:1 molar equivalent of sfGFP::Car9-K8AK11A with 10 nm SiNP at pH 7.5 (A) and following pH adjustment to 8.5 with NaOH (B).

Table S1: Mean hydrodynamic diameters (D_h) and full width at half max (FWHM) values of major scattering intensity peaks. Samples were prepared with a 5:1 molar equivalent of sfGFP::Car9-Car9 to 10 nm SiNP at pH 7.5 in the presence of the indicated concentrations of NaCl or KCl. DLS data was collected at pH 7.5 and following pH adjustment to 8.5.

Molarity (mM)	pH 7.5				pH 8.5			
	NaCl		KCl		NaCl		KCl	
	Mean D_h (nm)	FWHM (nm)	Mean D_h (nm)	FWHM (nm)	Mean D_h (nm)	FWHM (nm)	Mean D_h (nm)	FWHM (nm)
0	1210	1005	1210	1005	24	20	24	20
5	1340	950	1340	1032	44	25	44	32
10	1478	779	1524	1062	51	35	54	36
15	1718	1060	1940	1191	63	33	98	63
20	1963	1096	2335	1370	147	104	190	140
25	2480	1587	2688	1607	1280	380	1480	800
30	2868	1880	3261	2048	1990	950	2280	910

Table S2: Mean hydrodynamic diameters (D_h) and full width at half max (FWHM) values extracted from scattering intensity and particle number size distributions. The indicated bifunctional sfGFP constructs were mixed with 10 nm SiNP at a 5:1 molar equivalent of proteins to nanoparticles and DLS data was collected at pH 7.5 and following pH adjustment to 8.5.

Protein Name	pH 7.5				pH 8.5			
	Intensity		Number		Intensity		Number	
	Mean Dh	FWHM	Mean Dh	FWHM	Mean Dh	FWHM	Mean Dh	FWHM
sfGFP::Car9-Car9	1200	1006	1180	880	24	20	24	18
sfGFP::Car9-K8AK11A	150	126	143	73	23	18	23	21
sfGFP::K8AK11A-Car9	450	335	438	310	24	19	24	17
Car9-sfGFP::Car9	620	505	615	298	24	18	24	16

References

- 1 X. Qi, Y. Zhao, K. Lachowski, J. Boese, Y. Cai, O. Dollar, B. Hellner, L. Pozzo, J. Pfaendtner, J. Chun, F. Baneyx and C. J. Mundy, *ACS Nano*, 2022, **16**, 1919–1928.
- 2 B. Hellner, S. Alamdari, H. Pyles, S. Zhang, A. Prakash, K. G. Sprenger, J. J. De Yoreo, D. Baker, J. Pfaendtner and F. Baneyx, *J. Am. Chem. Soc.*, 2020, **142**, 2355–2363.